AFRL-SR-BL-TR-00-

REPORT DOCUMENTATION PAGE

0113

1. REPORT DATE (DD-MM-YYYY)	2. REPORT ~~DATE~~ TYPE	3. DATES COVERED (From - To)
3-16-2000	Final Report	3-1-1995 to 2-31-1998

4. TITLE AND SUBTITLE

Structure-Function Studies of Native and Recombinant Fish Antifreeze Proteins

5a. CONTRACT NUMBER

5b. GRANT NUMBER

F49620-95-1-0205

5c. PROGRAM ELEMENT NUMBER

6. AUTHOR(S)

Chi-Hing Christina Cheng-DeVries

Arthur L. DeVries

5d. PROJECT NUMBER

5e. TASK NUMBER

5f. WORK UNIT NUMBER

7. PERFORMING ORGANIZATION NAME(S) AND ADDRESS(ES)

University of Illinois
Dept. of Molecular & Integrative Physiology
524 Burrill Hall, 407 S. Goodwin Ave.
Urbana, IL 61801

8. PERFORMING ORGANIZATION REPORT NUMBER

9. SPONSORING/MONITORING AGENCY NAME(S) AND ADDRESS(ES)

10. SPONSOR/MONITOR'S ACRONYM(S)

11. SPONSORING/MONITORING AGENCY REPORT NUMBER

12. DISTRIBUTION AVAILABILITY STATEMENT

Unrestricted, Unclassified

13. SUPPLEMENTARY NOTES

14. ABSTRACT

This project investigates the structures of several fish antifreeze proteins, and how they interact with ice crystals and inhibit ice growth. Formation of hexagonal pit formation on ice crystal basal plane in the presence of fish antifreeze proteins was examined with two-photon fluorescence imaging which showed binding of antifreeze glycoprotein molecules on pit faces; the origin of pit development presumably stems from antifreeze adsorption on dislocations on the basal plane. A novel ice-active protein was isolated from AFGP-bearing notothenioid fish and its partial structure was determined. This protein and AFGP together lead to synergistic augmentation of antifreeze activity and thus has potential bearing on the design of more potent anti-freezing systems. A putative new type of antifreeze peptide was isolated from an Arctic liparid fish and its partial sequence was determined. And lastly, the X-ray crystallographic structure of a type III antifreeze peptide from an Antarctic eel pout and the protein's ice-binding surface were determined.

15. SUBJECT TERMS

Fish, antifreeze proteins, crystal structure-function, ice

16. SECURITY CLASSIFICATION OF:			17. LIMITATION OF ABSTRACT	18. NUMBER OF PAGES	19a. NAME OF RESPONSIBLE PERSON
a. REPORT	b. ABSTRACT	c. THIS PAGE			C.-H. Chris Cheng-DeVries
U/U	U/U	U/U	U/U	12	19b. TELEPONE NUMBER (Include area code) (217)333-4245

with the lattice match model between antifreeze and ice for hydrogen bonding to take place. The alignment direction of the large AFGPs 1-5 is also along a-axes but with more complexity. The large AFGPs 1-5 are more potent antifreeze than the small AFGPs, i.e. the activity in terms of the amount of non-colligative freezing point depression or thermal hysteresis, is larger. This is also manifested in their differential inhibitory effect on ice growth at temperatures within the thermal hysteresis gap (~ 0 °C to –1°C for pure AFGP solutions) at the same concentrations (w/v). In the presence of sub-physiological concentrations (5 mg/ml) of the small AFGPs 7-8, a single ice crystal can undergo limited ice growth within the hysteresis gap until the ice crystal reaches the shape of a hexagonal bipyramid. This indicates that growth along both the a-axes and the c-axis is not completely stopped by the small AFGPs at this concentration. In the presence of the large AFGPs 1-5, there is no hexagonal bipyramidal growth, but hexagonal pits (Fig. 2) appear on the basal plane indicating presence of some amount of basal plane growth, i.e. growth along c-axis, but a-axes growth is completely stopped. The basal plane growth completely halts when the basal plane becomes fully pitted.

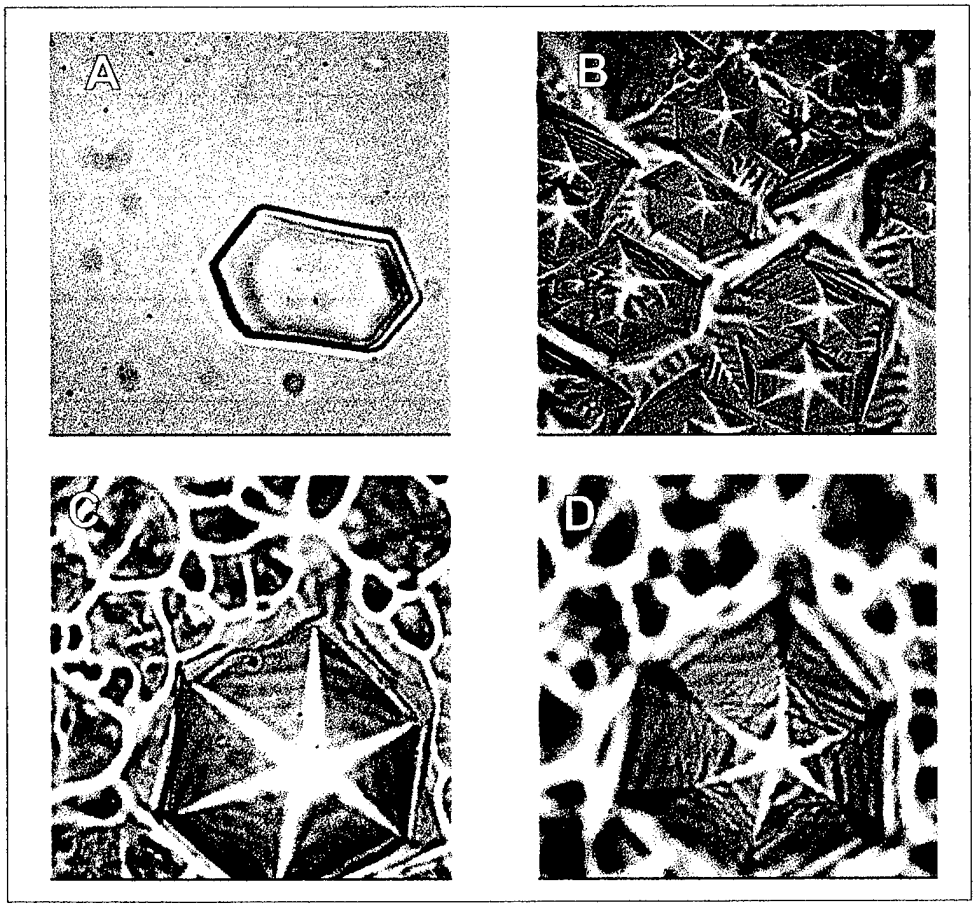

Fig. 2 Light microscope images. (A) Single hexagonal ice crystal showing basal plane, and C-axis is perpendicular to the paper. (B) Hexagonal pits form on basal plane of (A) held at –0.5°C in the presence of AFGPs 1-5. Steps are visible on the pit faces. (C) A single pit with focus at the top of the pit. Pit width from vertex to opposite vertex is about 80 uM, and depth is about 40 uM. (D) Same pit in (C) with focus at the bottom of the pit and showing growth steps on pit faces.

The appearance of complex growth steps on the pit faces suggests that there are particular ice crystallographic orientations where the large AFGPs bind to. To investigate the distribution of the AFGP molecules in the pit, as well as more detailed 3-dimensional structural information of the pits, we conducted imaging studies using fluorescently labeled AFGPs1-5 and two-photon fluorescence microscopy. AFGPs 1-5 were reacted with fluorescamine at room temperature, which labeled the alpha-amino group at the N-terminus, and purified from excess fluorescamine by Sephadex G-25 column chromatography. The two-photon microscopy set up is shown in Figure 3.

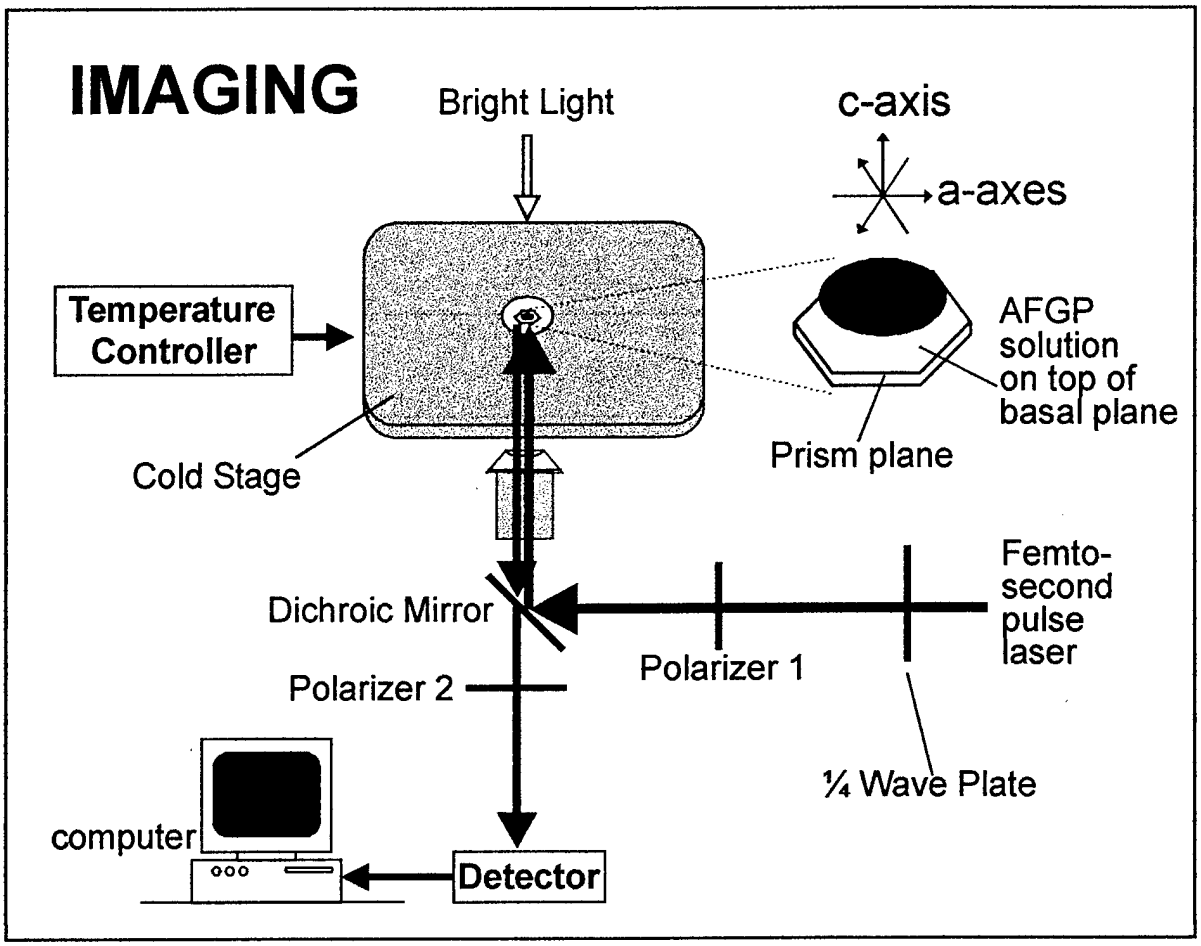

Fig. 3 Schematics of bright-light and two-photon microscopic imaging of AFGP 1-5 solution on single ice crystal.

For bright field light microscopy, light source is white light with no polarizers, and image capture was carried out with a CCD camera interfaced with the computer. For two-photon fluorescence measurements, a femto-second pulse laser provides pulse light of wavelength 750 nM, which is twice the maximum excitation wavelength of the conjugated fluorescamine. A piezoelectric motor was used for z-direction movement of the lens to obtain a series of images of the pits for 3-dimensional reconstruction. Fluorescence was measured with or without the polarizers in the light

path. Measurements without polarizers measure total emission from both bound or unbound AFGPs. Measurements with polarizers remove random emission of unbound AFGPs, and the polarization image represents fluorescence of adsorb AFGP molecules on ice along a specific directions. The polarized light intensity of the image is calculated with the equation:

$$P = (I_1 - I_2)/(I_1 + I_2)$$

where (I_1) and (I_2) are light intensities measured when the polarizers are parallel or perpendicular to each other. Three-dimensional structure of the pits was reconstructed using the software Spyglass. Figure 4 shows several of the images of pit cross sections serially obtained at 5 uM intervals without polarizers.

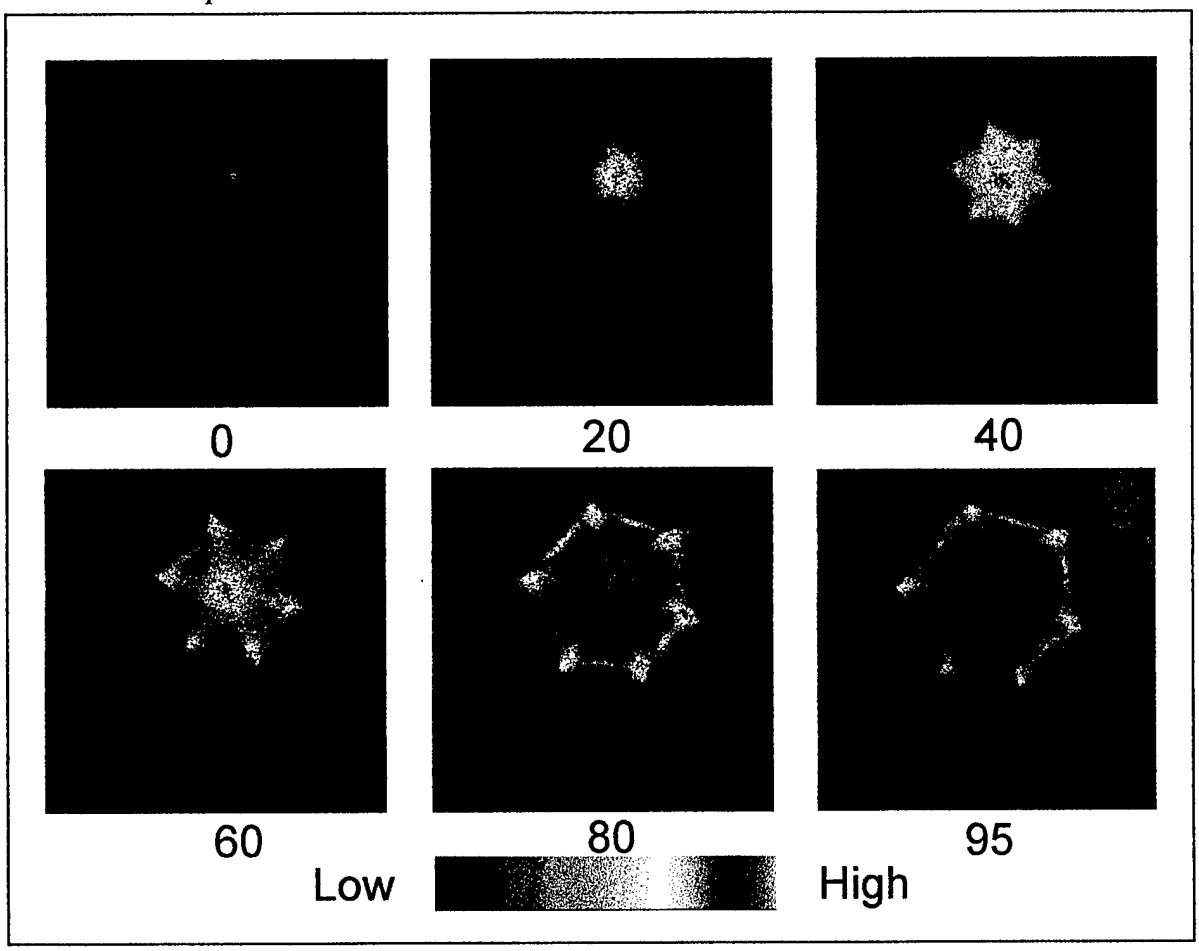

Fig. 4 Cross-sectional fluorescence images of a hexagonal pit separated. The numbers indicate distance from bottom of pit in uM. Image intensity has been normalized to a standard. Black is unpitted ice. Blue to red represents increasing concentration of AFGPs.

The AFGP molecules appear to be highly concentrated/bound at the corners of the pit and to some extent on the pit faces. The high concentration in the center of the pit for sections up to 60 uM from the bottom may represent a pool of AFGP solution in the pit cavity rather than specific binding. To ascertain this, vertical 3-dimensional structure of the pit was constructed, and shown in Figure 5.

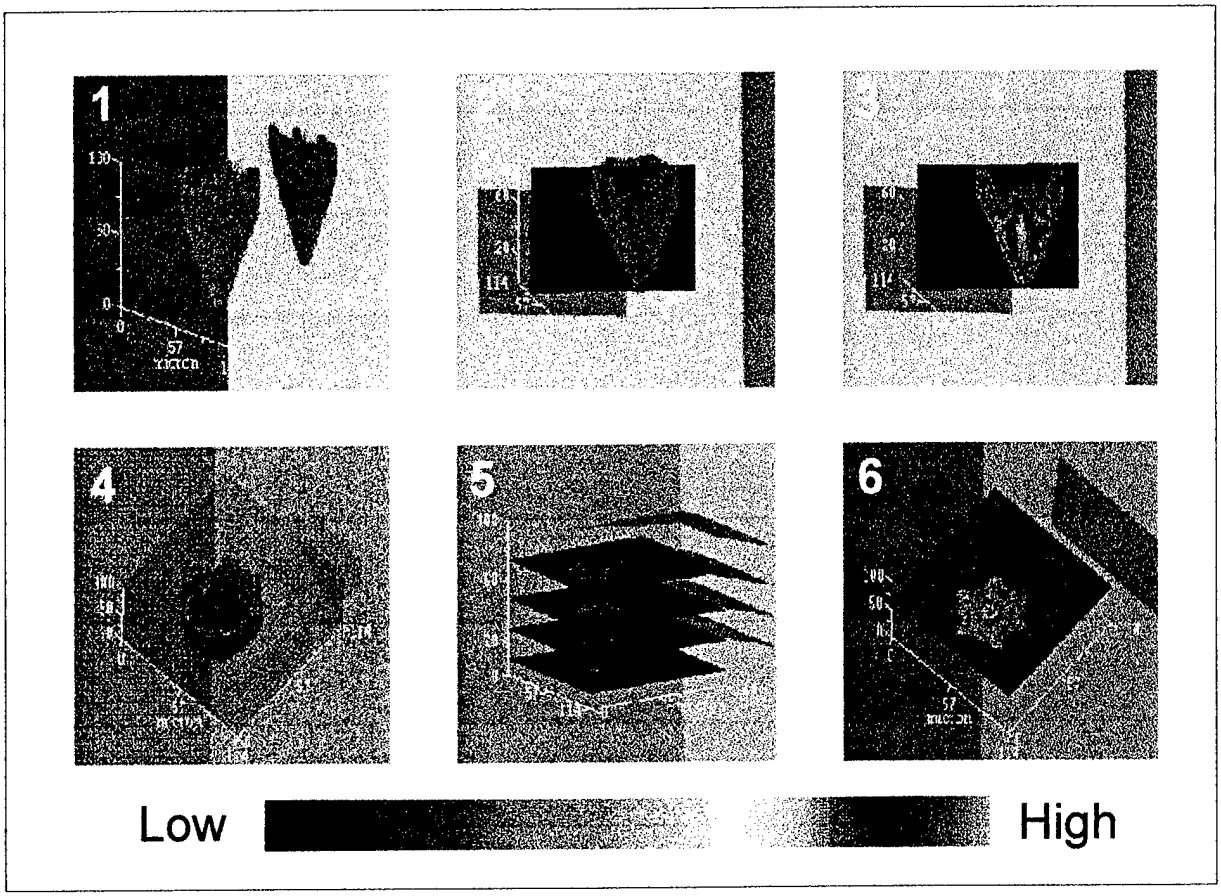

Fig. 5 Computer generated reconstruction of three-dimensional structure of a pit from from images of cross and longitudinal sections.

The 3-D structure of a "fully-grown" pit shows that it has the dimension of about 80 uM deep by 40 uM across two opposite vertices at the top. The angle made by two opposing pit faces (panels 1, 2 and 3) was calculated to be $42\pm2^{\circ}$. The longitudinal section of the pit (panel 3) shows that the AFGP fluorescence is consistently high down the whole length of the pit faces, in keeping with AFGP fluorescence at the corners and along the hexagonal perimeter (panel 6), and indicating AFGP binding at sites. The presence of high fluorescence intensity in the bottom half of the pit cavity and the absence of it on the top half may be due to the limited surface area for AFGP adsorption at the narrow pit bottom leaving more AFGPs in the bulk solution, and vice versa at the top.

To determine if the adsorbed AFGP molecules are all aligned in a specific direction, fluorescent polarization image of pits were obtained, and shown in Figure 6. The polarized fluorescence measurements from the pits (panel 3) remove the random emission of unbound AFGPs in bulk solution (panels 1 and 2). The polarized intensity is much reduced but is clearly present, indicating that AFGPs are adsorbed at the ice-water interface and possibly aligned along a given direction. However, the resolution of the images is not high enough for definitive determination of the alignment.

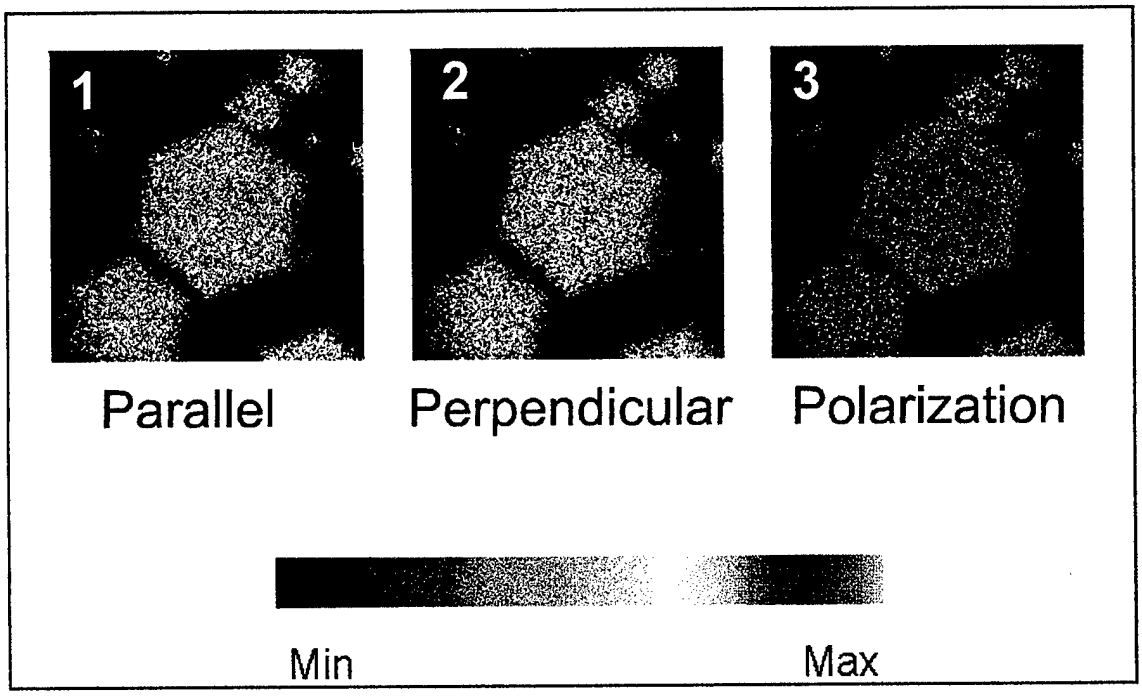

Fig. 6 Images of pits taken with the two polarizers parallel (1) and perpendicular (2) to each other. The polarization image intensity (3) was calculated by the equation: $P = (I_1 - I_2)/(I_1 + I_2)$.

Fish antifreezes except the small AFGPs 7-8 cause pitting of the basal plane of single crystal ice at temperatures within the hysteresis gap. The expression of the pit faces and the steps within suggested that the antifreeze molecules adsorbed to those faces and retard their growth, thus leading to their expression. Using fluorescently labeled large AFGPs 1-5, the above series of studies experimentally demonstrated adsorption of the antifreeze molecule to the ice surface of the pits. It is not known what is the origin of the pit development, presumably it begins with AFGP adsorption to dislocations in the ice crystal lattice. Parallel situations likely exist for the other antifreezes. The general conclusion is thus, within the hysteresis gap, antifreezes (except AFGPs 7-8) inhibit prism plane growth but allow limited growth on the basal plane resulting in pit formation as layers of C-axis growth occur, and when basal plane becomes fully pitted, ice growth completely stops.

A NOVEL ANTIFREEZE POTENTIATING PROTEIN - AFPP

In our attempt to isolate a putative novel antifreeze reported in the literature from the Antarctic silverfish, *Pleurogramma antarcticum*, we found instead a second ice-active protein that potentiates the activity of AFGPs, the primary antifreeze component in the notothenioid fishes. AFPP was purified from the AFGPs in the serum by precipitation with 40% ammonium sulfate (AFGP stays in the supernatant), following by Sephadex column chromatography which fractionates AFPP from other serum proteins. AFPP occurs at much lower physiological concentration than AFGPs, and by itself produces very small amount of hysteresis, but augments the activity of AFGP1-5 (the large

isoforms) substantially above additive levels. Pure AFPP or AFGP1-5 at 1 mg/ml alone has 0.2°C of thermal hysteresis, but when combined, the two proteins produce a total activity of 1.1°C to 1.4°C. For this reason, the novel protein is named antifreeze potentiator protein. The amount of activity enhancement is inversely proportional to the size of the test ice crystal; the smaller the seed ice, the greater the total hysteresis. Interestingly AFPP does not appear to enhance the activity of the smaller isoforms, AFGP6, 7 and 8. We have purified and partially characterized AFPP from *P. borchgrevinki.* It is a relatively small peptide of 15,489 Da, and we have obtained its partial sequence:

NH_2-AGTENSAGPQVAFSAGLSDAG------R/KLLFPVSAGQDK------R/KFNMW-COOH

It is interesting that the are four repeats of the dipeptide, Ala-Gly (red), in the first 20 residues alone, and appears again in one of the tryptic fragments. The amino acid composition shows that there are equal numbers of Ala and Gly in the protein, suggesting that this may be a repetitive motif the protein. Ala and Gly have helix making potential, and thus if this dipeptide is repeated, the protein may have helical structure, or contains a helical domain. Preliminary circular dichroism appears to indicate the presence of some percentage of helical secondary structure.

The ability of the potentiator protein to augment antifreeze activity of the AFGPs by conferring the property of ice crystal size dependency suggest possibilities of greater function in this two protein system, that may be exploited for application. Preliminary results from single ice crystal hemisphere grown from AFPP followed by etching suggest that AFPP may be adsorbing to the basal plane. While different fish antifreezes preferentially adsorb to different ice crystallographic planes, none has been found to adsorb on the basal plane, thus permitting limited C-axis growth within the hysteresis gap demonstrated in the prior section. The synergistic effect on antifreeze activity in the presence of both AFPP and AFGP may be related to the basal plane adsorption of AFPP, resulting in complete inhibition of both a-axes and C-axis growth in this two protein system.

A PUTATIVE NEW TYPE OF ANTIFREEZE PEPTIDE FROM AN ARCTIC LIPARID FISH

We have isolated antifreeze peptides (AFP) from an Arctic liparid fish, *Liparis liparis*, which may prove to be a new type of AFP. AFPs were purified from fish serum by Sephadex G75 size fractionation column chromatography followed by RP-HPLC (Reverse Phase High Pressure Liquid Chromatography). RP-HPLC shows that there are 3 prominent AFP variants, LST-C, LST-D, and LST-E. The major variant, LST-C, was being characterized. N-terminal sequencing produced 69 residues. MS-MS (quadrupole Mass spectrometry) sequencing of LST-C tryptic and Asp-N fragments were carried out to determine the C-terminus sequence. The alignment of the tryptic and Asp-N fragments with the sequence from N-terminal sequencing of native LST-C is given below:

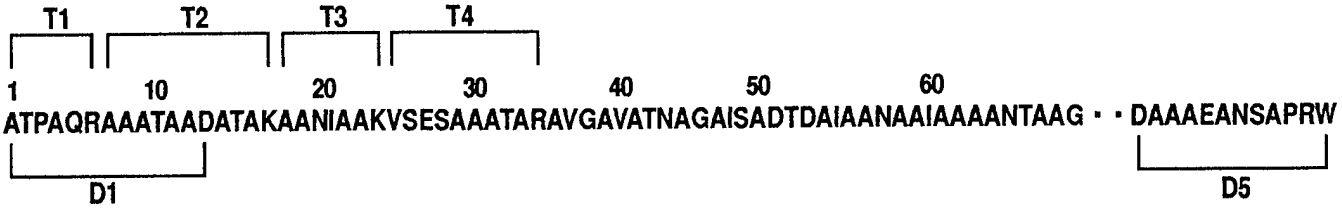

The high Ala content (53%) of LST-C suggests that it might have substantial helical structure, and indeed circular dichroism data showed it to be so. The calculated helical content is about 35% to 50% helix when measured at -0.5°C and a concentration of 100 μM.

Characterizing the structures of newly found antifreezes, whether the antifreeze resembles a known type or is a novel type in itself, is useful in the study of structure-function relationship of antifreeze proteins in that the additional structural information may either confirm existing theories or data, or provide alternate possibilities as to how antifreeze proteins interact with ice to produce the observed function. The current results of liparid AFP LST-C shows that, like type I AFP of flat fishes it is rich in Ala and alpha-helical in secondary structure. But unlike type I AFP, it is twice as large, 7.5 kDa versus the 3.5-4.5 kDa of known type I AFPs, and that it does not have the characteristic 11-residue repeats (Ala8-aa2-Thr) which are found to be important in forming a stable alpha-helix and placing the Thr in almost colinearity for binding to ice. Ultimately determining the LST-C's 3-D structure and how it interacts with ice will further our understanding of the helical AFPs in general.

THREE-DIMENSIONAL STRUCTURES OF TYPE III AFPS

Type III AFPs from the related Antarctic eel pouts and Atlantic ocean pouts are small globular proteins of about 7 kDa, unbiased in amino acid composition and without repeat sequence motifs. Thus the lattice match model of ice-binding, i.e. alignment of regularly spaced putative ice binding moieties in the protein and periodic water molecules in the ice lattice, does not appear to apply. To understand how type III AFP binds to ice, we have obtained the 3-D structure of the major type III AFP, AB1 (7 kDa), from the Antarctic eel pout *Austrolycicthys* (*Pachycara*) *brachycephalum* by 2-dimensional Nuclear Magnetic Resonance Spectroscopy, as well as 3-D structures of several naturally-occurring type III AFP variants from a closely related Antarctic eel pout, *Lycodicthys dearborni*, for comparison. The rationale is that these closely related AFP variants (differ by 2- 8 residues) represent a set of natural "mutants" which have been evolved and refined in nature to perform the same function, and thus comparative examination of their structures may shed light on the common structural elements that confer the function. *Lycodicthys dearborni* has 3 major AFPs, two of them, LD1 and LD2 are like AB1 in sequence and size (7 kDa), and the third, LD3, is 14 kDa and comprised of two 7 kDa AFP domains of similar sequence to the 7 kDa variants linked by a 9-residue unique sequence. Th sequences of these AFPs and the AFP from the related Atlantic ocean pout (OP) are:

```
                    *   *                    *
AB1    TKSVVASQLIPINTALTPAMMKAKEVSPKGIPAEEMSKIVGMQVNRAVNLDETLMPDMVKTYQ
LD1   NKASVVANQLIPINTALTLIMMKAEVVTPMGIPAEEIPKLVGMQVNRAVPLGTTLMPDMVKNYE
LD2   NKASVVANQLIPINTALTLIMMKAEVVTPMGIPAEDIPRIIGMQVNRAVPLGTTLMPDMVKNYE

LD3   NKASVVANQLIPINTALTLIMMKAEVVTPMGIPAEEIPNLVGMQVNRAVPLGTTLMPDMVKNYE- DGTTSPGLK-
         SVVANQLIPINTALTLVMMKAEEVSPKGIPSEEISKLVGMQVNRAVYLDQTLMPDMVKNYE
OP     SQSVVATQLIPMNTALTPAMMEGKVTNPIGIPFAEMSQLVGKQVNTPVAKGTLMPNMVKTYAA
```

The x-ray crystallography studies are carried out in collaboration with Dr. Andrew Wang and Dr. Howard Robinson in the Dept. of Cellular and Structural Biology at the University of Illinois. All three AFPs of *L. dearborni,* LD1, LD2 and LD3 formed crystals readily in 30% PEG-4000 and 0.2M ammonium sulfate. Large crystals were then grown in larger dips and crystals ranging in size from 0.5 to 1 mm were obtained.

Crystals of all three AFPs were mounted and room temperature diffraction data were collected to about 1.5A. The crystals were also mounted at -150°C and diffraction data were collected to 1.2A. The crystal phasing was solved by isomorphous molecular replacement from the NMR coordinates of AB1. The LD1 model was then refined against the observed data to a R-Factor of 17.5% with only isotropic atomic B-factor refinement. The average atomic B-factor for the LD1 protein model is 7.5 for the data set collected at -150°C. The model for RD2 has been refined to a R-factor of 19.8% with two conformations for Met30, Met43 and Leu55. The LD2 model also includes one TRIS buffer cation and 139 water molecules and the average atomic B-factor for the protein atoms is 12.7 for the data set collected at -150°C.

The refinement of the two-AFP-domain LD3 is more complex in that in the two, some type of disorder exists in the crystal. The sequences of the two AFP domains of LD3 are very similar. For the LD3 crystal, the data show that the unit cell is nearly identical to LD1 or LD2. Thus, the data are consistent with both domains occupying the same space half of the time due to disorder in the crystal. The data have been refined consistent with this disorder. We are now currently investigating methodologies for decomposing this data such that a single complete model can be produced which will be consistent with the observed data.

The stereogram below (Fig. 7) shows the refined LD1 model. The electron density map is of the conserved surface amino acids from the face labeled I in the stereogram. A space filled 3-D structure of LD1 is shown (Fig. 8) with the face I showing residues (red) that may be involved in ice-binding.

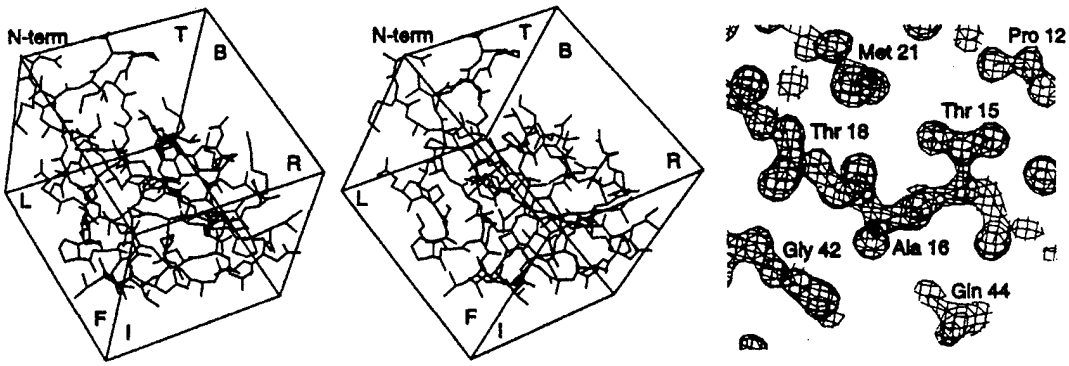

Fig. 7 Stereogram of 7 kDa type III AFP, LD1, from an Antarctic eel pout.

Qualitatively, the overall shape of the 7 kDa type III AFPs are rather cubic with one corner "sliced off". In other words, it has several rather flat surfaces that may act as the binding surface

to ice. The face I contains surface amino acids that are conserved in the four AFPs under study here as well as in the type III AFP of the related north Atlantic ocean pout.

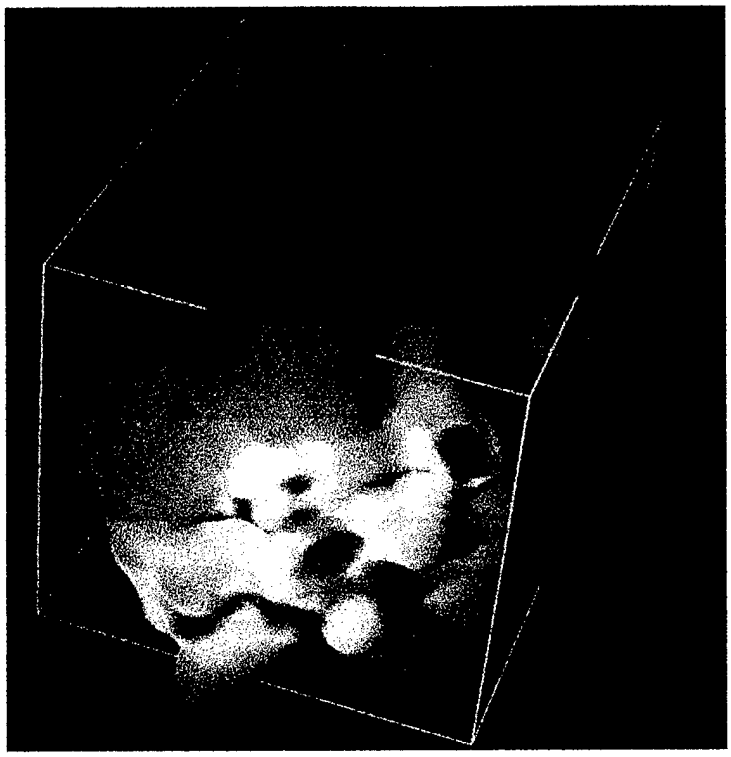

Fig. 8 Space-filled 3-D structure of type III AFP, LD1, from an Antarctic eel pout showing the putative ice-binding face (I) and the putative ice-binding residues (red).

It has been suggested that for the ocean pout AFP (OP-AFP), 3 polar residues, Asn13, Thr17 and Gln43 may be important in conferring antifreeze activity through site directed mutagenesis. These 3 residues are conserved in AB1, LD1, LD2 and in each of the two AFP domains of the 14 LD3 (marked with * in the sequences above), and occur in face I. Molecular modeling of these AFP on ice crystal shows that this face and the three conserved residues could dock on the inner corner between the prism face and basal plane of the ice lattice. However, currently, there are no unequivocal evidence for a specific ice crystallographic site where type III AFPs bind to. The single ice crystal etching experiments in collaboration with Dr. Charles Knight at National Center of Atmospheric Studies, which thus far comprised the only approach for determining the crystallographic orientation of antifreeze protein adsorption, have produced very complex type III AFP etch patterns in single crystal ice that are difficult to interpret. The adsorption appeared to be on the prism face of ice crystal but also included a spread of interfacial orientations. In addition there are differences between the etch pattern of AB1 versus that of LD1 even though the two are 80% identical in sequence. However, the etch pattern between LD1 (single AFP domain) and LD3 (two AFP domains) are very similar.

Of the four known types of antifreeze proteins, three of them, the AFGPs, type I AFP and type III AFP are similar in their potency in inhibiting ice crystal growth at the same concentrations (w/v), while type II AFP is much less effective. The ice absorption mechanisms of the helical AFGPs and type I AFP are now fairly well understood, but not for that of the globular type III AFP. Type III AFP however is a good candidate for potential practical applications because it can be effectively produced by biotechnological methods because of its ideal size and non-biased amino acid composition for bacterial expression. Biotechnological production of AFGPs is limited by lack of current technology to glycosylate the peptide backbone appropriately, and that of type I AFP is limited by its small size which is prone to bacterial proteolysis and solubility problems due to its high alanine content. Thus elucidating the ice adsorption mechanism of type III AFP not only adds to fundamental understanding of the action of biological antifreezes, it is also pertinent in that it may allow rationale designs be made on a simple molecule that is ideal for expression through biomolecular routes.

However, the mechanism of ice adsorption of type III AFP proved to be more complex than the helical AFGPs and type I AFPs. The observations on the adsorption characteristics of type III AFP to single-crystal ice are extremely complex, and currently no conclusive interpretations can be made yet in terms of the orientation of adsorption or alignment direction of the antifreeze molecules. Several approaches are being considered for resolving these complexities. The importance of face I and any other flat faces of the AFP molecules in binding to ice will be tested by systematically attaching large molecules (not by modifying the intrinsic amino acid but linking to non-protein organic molecules). To determine the ice crystallography of the adsorption of these AFPs etching experiments of single crystal ice hemispheres grown from lower concentrations of AFPs may yield a clearer internal etching pattern. Observations of the morphology of the advancing growth surface of single-crystal ice grown from dilute antifreeze solution will also be made using light microscopy. The crystallographic morphology at a finer scale may also shed light on the adsorption orientation of the type III AFPs, like the case of the AFGPs we previously determined.

PERSONNEL SUPPORTED OR ASSOCIATED WITH PROJECT

Chi-Hing Chris Cheng-DeVries, Ph.D. Senior Research Scientist (Physiology) University of Illinois	Co-principal investigator, 100% time
Arthur L. DeVries, Ph.D. Professor of Physiology University of Illinois	Co-principal investigator, 0% time
Yumi Jin Department of Physiology University of Illinois	Graduate Student, 50% time
Gerry Paik Department of Physiology University of Illinois	Undergraduate research assistant, 3 summer months
Andrew Wang, Ph.D. Professor of Cellular and Structural Biology University of Illinois	Collaborator-X-ray crystal structure antifreeze protein
Tony Haymet, Ph.D. Professor of Chemistry University of Sidney Australia	Collaborator-antifreeze structures computations and modeling
Charles Knight, Ph.D. NCAR Boulder, Colorado	Collaborator-ice crystallography of antifreeze adsorption
Karl Eric Zachariassen, Ph.D. Professor of Biology University of Trondheim Norway	Collaborator-ice crystal size dependency of the novel antifreeze protein from Antarctic silverfish